JPn Neuroscience

The Journal of Physiology

J Physiol 591.1 (2013) pp 203–217

Direct and GABA-mediated indirect effects of nicotinic ACh receptor agonists on striatal neurones

Ruixi Luo, Megan J. Janssen, John G. Partridge and Stefano Vicini

Department of Pharmacology and Physiology and Interdisciplinary Program in Neuroscience, Georgetown University School of Medicine, Washington, DC 20007, USA

Key points

- Pharmacological activation of nicotinic ACh receptors (nAChRs) excites striatal interneurones and induces a GABA-mediated current in medium spiny projecting neurones (MSNs) via feedforward inhibition.
- Striatal interneurones identified as neuropeptide Y $(NPY)^+$, parvalbumin $(PV)^+$ and tyrosine hydroxylase $(TH)^+$ have somatic expression of nAChRs.
- The neurogliaform (NGF) subtype of NPY^+ interneurones exhibits the most robust nicotinic response and has high synaptic connectivity with MSNs.
- Antagonism of nAChR responses suggests the expression of distinct receptor subtypes between interneurone classes.
- NPY^+ NGF and TH^+ interneurones mediate cholinergic control of MSNs and thus striatal output via $GABA_A$ receptors.

Abstract Choline acetyltransferase-expressing interneurones $(ChAT)^+$ of the striatum influence the activity of medium spiny projecting neurones (MSNs) and striatal output via a disynaptic mechanism that involves GABAergic neurotransmission. Using transgenic mice that allow visual identification of MSNs and distinct populations of GABAergic interneurones expressing neuropeptide Y $(NPY)^+$, parvalbumin $(PV)^+$ and tyrosine hydroxylase $(TH)^+$, we further elucidate this mechanism by studying nicotinic ACh receptor (nAChR)-mediated responses. First, we determined whether striatal neurones exhibit pharmacologically induced nicotinic responses by performing patch-clamp recordings. With high $[Cl^-]_i$, our results showed increased spontaneous IPSC frequency and amplitude in MSNs as well as in the majority of interneurones. However, direct nAChR-mediated activity was observed in interneurones but not MSNs. In recordings with physiological $[Cl^-]_i$, these responses manifested as inward currents in the presence of tetrodotoxin and bicuculline methobromide. Nicotinic responses in MSNs were primarily mediated through $GABA_A$ receptors in feedforward inhibition. To identify the GABAergic interneurones that mediate the response, we performed dual recordings from GABAergic interneurones and MSNs. Both TH^+ and neurogliaform subtypes of NPY^+ (NPY^+ NGF) interneurones form synaptic connections with MSNs, although the strength of connectivity, response kinetics and pharmacology differ between and within the two populations. Importantly, both cell types appear to contribute to nAChR-mediated GABAergic responses in MSNs. Our data offer insight into the striatal network activity under cholinergic control, and suggest that subclasses of recently identified TH^+ and

R. Luo and M. J. Janssen have contributed equally to this work.

DOI: 10.1113/jphysiol.2012.241786

NPY$^+$ interneurones are key mediators of striatal nicotinic responses via GABAergic tonic and phasic currents.

(Received 27 July 2012; accepted after revision 2 October 2012; first published online 8 October 2012)

Corresponding author S. Vicini: Department of Pharmacology and Physiology, Basic Science Building, Rm 225, Georgetown University School of Medicine, 3900 Reservoir Rd, Washington, DC 20007, USA. Email: svicin01@georgetown.edu

Abbreviations AChE, acetylcholinesterase; ACSF, artificial cerebrospinal fluid; Atr, atropine; BMR, bicuculline methobromide; ChAT, choline acetyltransferase; CCh, carbachol; DHβE, dihydro-β-erythroidine; EGFP, enhanced green fluorescent protein; MLA, methyllycaconitine; MSNs, medium spiny projecting neurones; nAChRs, nicotinic ACh receptors; NBQX, 1,2,3,4-tetrahydro-6-nitro-2,3-dioxo-benzo[f]quinoxaline-7-sulphonamide disodium salt hydrate; NGF, neurogliaform; NPY, neuropeptide Y; PLTS, persistent low-threshold spiking; PV, parvalbumin; RMP, resting membrane potential; sIPSC, spontaneous IPSC; TH, tyrosine hydroxylase; TTX, tetrodotoxin.

Introduction

Intrinsic striatal mechanisms that regulate the excitability of medium spiny projecting neurones (MSNs) are of crucial interest in understanding the underlying factors that regulate movements, and may be important as pharmacological targets in the treatment of striatal disorders. Recently, we and others have reported the occurrence of tonic GABAergic inhibition in MSNs (Ade *et al*. 2008; Janssen *et al*. 2009, 2011; Santhakumar *et al*. 2010). These studies have confirmed that tonic GABAergic conductance, mediated by high-affinity $GABA_A$ receptors, regulates MSN excitability. MSNs project either to the substantia nigra pars reticulata through a direct pathway or the globus pallidus through an indirect pathway (Gerfen *et al*. 1990). Proper motor control relies on a balance of these pathways, which becomes disrupted in dopamine-depletion animal models of Parkinson's disease, along with altered MSN excitability and synchrony (Fino *et al*. 2007; Azdad *et al*. 2009; Burkhardt *et al*. 2009; Jáidar *et al*. 2010). Choline acetyltransferase (ChAT)$^+$ interneurones shape striatal output and reward-associated behaviours (Graybiel *et al*. 1994; Calabresi *et al*. 2000; Pisani *et al*. 2007; Sullivan *et al*. 2008; Drenan *et al*. 2010; Witten *et al*. 2010; Bonsi *et al*. 2011; English *et al*. 2011). Activation of these interneurones has been shown to indirectly increase synaptic GABA events in MSNs through GABAergic interneurones (de Rover *et al*. 2002; Sullivan *et al*. 2008; Witten *et al*. 2010; English *et al*. 2011). These results suggest a preferential activation of specific GABAergic interneurones that mediate striatal cholinergic regulation.

Recently, a subclass of neuropeptide Y (NPY)$^+$ interneurones identified as neurogliaform (NGF) has been characterized in the striatum, and has been shown to be crucial in mediating striatal cholinergic regulation (English *et al*. 2011; Ibáñez-Sandoval *et al*. 2011). This evidence suggests that MSN GABAergic tonic conductance may have cholinergic origin. In the striatum approximately 1% of cells are tonically active. Among them NPY$^+$, tyrosine hydroxylase (TH)$^+$ and ChAT$^+$ cells have been shown to exhibit spontaneous activity in acute striatal slices (Bennett & Wilson, 1999; Zhou *et al*. 2002; Dehorter *et al*. 2009; Partridge *et al*. 2009; Gittis *et al*. 2010; Ibáñez-Sandoval *et al*. 2010; Beatty *et al*. 2012). ChAT$^+$ interneurones have large somas and extensive axonal branching (Wilson *et al*. 1990), making them well positioned to exert strong cholinergic influence locally via production of an indirect GABAergic tone. Direct application of nicotinic agonists has been reported to generate inward currents or depolarize certain classes of striatal interneurones (de Rover *et al*. 2002; Koós & Tepper, 2002; English *et al*. 2011). Using transgenic mice that allow fluorescent identification of MSNs or distinct populations of striatal GABAergic interneurones expressing parvalbumin (PV)$^+$, TH$^+$ and NPY$^+$, we performed patch-clamp recordings to investigate neuronal selective expression of nicotinic receptors and to verify the occurrence of a cholinergic driven GABAergic tone. We also performed dual recordings to further investigate GABAergic control of MSNs that arise from persistent cholinergic activation of the striatal network. Understanding the relationship between these two crucial neurotransmitter systems will unravel fundamental aspects of the striatal network and can provide important pharmacological targets in the treatment of striatal disorders.

Methods

Slice preparation

Brain slices were prepared from young male and female mice (P15–21). The following mice were used: bacteria artificial chromosome (BAC) *drd2*-enhanced green fluorescent protein (EGFP); *drd1a*-tdTomato (GENSAT; Gong *et al*. 2003; Shuen *et al*. 2008), BAC-NPY (*npy* promoter attached to a humanized Renilla GFP Stock 006417; Jackson Laboratory, Bar Harbor, ME, USA), PV-Cre;ROSA-tdTomato (Madisen *et al*. 2010; Murray *et al*. 2011) and TH-EGFP (Ibáñez-Sandoval *et al*. 2010;

Tg(Th–EGFP) stock obtained from MMRC strain #292). Mice were killed by decapitation in agreement with the guidelines of the AMVA Panel on Euthanasia and the Georgetown University animal care and use committee. The whole brain was removed and placed in an ice-cold slicing solution containing (in mM): NaCl, 85; KCl, 3; $CaCl_2$, 0.5; $MgSO_4$, 7; NaH_2PO_4, 1.25; $NaHCO_3$, 25; glucose, 25; sucrose, 75 (all from Sigma, St Louis, MO, USA). Corticostriatal coronal slices (250 μm) were prepared using a Vibratome 3000 Plus Sectioning System (Vibratome, St Louis, MO, USA) in ice-cold slicing solution. They were incubated in artificial cerebrospinal fluid (ACSF) containing (in mM): NaCl, 124; KCl, 4.5; Na_2HPO_4, 1.2; $NaHCO_3$, 26; $CaCl_2$, 2.0; $MgCl_2$, 1; dextrose, 10.0; at 305 mosmol l^{-1} at 32°C for 30 min. The slices then recovered for an additional 30 min in ACSF at room temperature, 23–25°C. All solutions were maintained at pH 7.4 by continuous bubbling with 95% O_2, 5% CO_2. During experiments, slices were completely submerged and continuously perfused (2–3 ml min^{-1}) with ACSF at room temperature.

Whole-cell recordings

Hemislices containing the cortex and the anterior striatum were visualized under upright microscopes (E600FN or FN1 Nikon, Japan) equipped with Nomarski optics and an electrically insulated 60× water immersion objective with a long working distance (2 mm) and high numerical aperture (1.0). In *drd2*-EGFP; *drd1a*-tdTomato mice, MSNs were classified as being either striatopallidal dopamine D2 receptor positive ($D2^+$) or striatonigral dopamine D1 receptor positive ($D1^+$) based on their expression of EGFP or tdTomato, respectively. In all other transgenic mice, MSNs were not tagged with fluorescent proteins, and the sample population likely contains both $D1^+$ and $D2^+$ MSNs. Neurones were visualized with green or red fluorescent protein, based on animal genotype, and often confirmed with firing patterns. Identification of fluorescent protein-expressing neurones was performed by epifluorescent excitation of the tissue with a mercury-based lamp and standard filter sets.

Recording pipettes 4–6 MΩ were pulled on a vertical pipette puller from borosilicate glass capillaries (Wiretrol II; Drummond, Broomall, PA, USA) and filled with either KCl or potassium gluconate-based internal solutions. The KCl-based internal solution contained (in mM): KCl, 145; Hepes, 10; ATP·Mg, 5; GTP·Na, 0.2; EGTA, 5; adjusted to pH 7.2 with KOH. In potassium gluconate-based internal solutions (labelled as 'Kgluc' in some figures), KCl was replaced with equimolar potassium gluconate and pH was adjusted with KOH.

Voltage-clamp recordings were performed using the whole-cell configuration of the patch-clamp technique at a holding voltage of −70 mV using the Multiclamp 700B amplifier (Molecular Devices, Sunnyvale, CA, USA). When Kgluc internal solutions were used, the baseline membrane potential for current-clamp recordings was set at −70 mV before each series of current step injection protocols. In a small subset of cells, we examined evoked excitatory postsynaptic currents via whole-cell voltage-clamp recordings (Partridge *et al.* 2009). Evoked responses were obtained using a twisted bipolar stimulating electrode placed near the white matter separating the cortex from the striatum. For these recordings, we used an internal solution containing (in mM): potassium gluconate, 145; Hepes, 10; BAPTA, 10; GTP.Na, 0.2; ATP.Mg, 5; and supplemented with 5 lidocaine *N*-ethyl bromide (QX-314), pH adjusted to 7.4 with KOH.

Stock solutions of bicuculline methobromide (BMR), carbachol (CCh), atropine (Atr), dihydro-β-erythroidine (DHβE), 1,2,3,4-tetrahydro-6-nitro-2,3-dioxo-benzo[f]quinoxaline-7-sulphonamide disodium salt hydrate (NBQX; Abcam Biochemicals Cambridge, MA, USA) cytisine (Abcam Biochemicals Cambridge, MA), mecamylamine (MEC Abcam Biochemicals Cambridge, MA), methyllycaconitine (MLA; Tocris Bioscience, Minneapolis, MN, USA) and tetrodotoxin (TTX; Alomone Labs, Israel) were prepared in water. All stock solutions were diluted to the desired concentration in ACSF and applied locally through a 'Y-tube' (Murase *et al.* 1989) modified for optimal solution exchange in brain slices (Hevers & Luddens, 2002). In most cases, multiple experiments were not performed on the same cell to avoid receptor desensitization.

Currents were filtered at 2 kHz with a low-pass Bessel filter and digitized at 5–10 kHz using a personal computer equipped with Digidata 1322A data acquisition board and pCLAMP10 software (both from Molecular Devices). Off-line data analysis, curve fitting and figure preparation were performed with Clampfit10 software (Molecular Devices). Spontaneous (s)IPSCs were identified using a semi-automated threshold-based mini-detection software (Mini Analysis, Synaptosoft Inc., Fort Lee, NJ, USA) and were visually confirmed. Event detection threshold was set at five times the RMS (root mean square) level of baseline noise. NBQX was not included in sIPSC measurements to not perturb the network activity. AMPA-mediated spontaneous EPSCs could easily be identified by the rapid decay kinetics (<8 ms), and were excluded from the IPSC analysis, as we have previously described (Ortinski *et al.* 2004; Forcelli *et al.* 2012). All detected events were used for event frequency analysis, but superimposing events were eliminated for the amplitude and decay kinetic analysis. AChR-mediated current was primarily measured with an all-points histogram that measured the mean holding current 10 s before and during drug application. Holding current changes during high-frequency stimulation of

synaptically connected pairs was assessed similarly after low-pass filtering (2–5 Hz).

Excised patch recordings

Recordings of single-channel activity were performed in excised outside-out patches held at −60 mV. Because it was rare to find patches with single channels, kinetic analyses were performed on stretches with few superimposed channel openings. Events for single-channel dwell time analyses were collected using half-amplitude threshold detection method built into pCLAMP 10 software, and >500 events were collected for all conditions. Superimposed openings were excluded. Mean unitary current was determined from the Gaussian fits of amplitude distributions of openings to the main conductance level lasting more than 0.5 ms.

Statistics

To sample a representative population, each variable examined in this study was derived from at least three different animals from at least two or more breeding pairs. Statistical significance was determined using the paired two-tailed Student's *t* test to compare pre-drug conditions with recordings made under drug conditions of the same cell population. One-way ANOVA for repeated measures followed by Tukey's *post hoc* test was used for comparisons across cell groups. All values in text and figures are expressed as mean ± SEM. In all summary graphs, the number of cells studied is in parentheses.

Results

The expression of fluorescent proteins under the control of cell-type-specific promoters allowed the selective identification of striatal interneurones. The identity of individual neurones was further confirmed by their response to hyperpolarizing and depolarizing current injections. As shown in Fig. 1, MSNs identified in *drd2*-EGFP; *drd1a*-tdTomato mice had medium-sized cell bodies, and were characterized by the presence of inward rectification and delayed firing (see Kreitzer, 2009 for review). In contrast, NPY^+ persistent low-threshold spiking (PLTS) interneurones in NPY-EGFP mice had larger soma and firing characteristics, as previously reported (Fig. 1; Kawaguchi *et al.* 1993; Koós & Tepper, 1999; Partridge *et al.* 2009; Ibáñez-Sandoval *et al.* 2011). However, when NPY^+ cells with brighter fluorescence, round soma and multiple primary dendrites were selected, we confirmed the recently reported findings of NGF neurones in the striatum (English *et al.* 2011; Ibáñez-Sandoval *et al.* 2011). NPY^+ NGF neurones displayed inward rectification and a regular firing pattern (Fig. 1*B*). Fast-spiking interneurones in PV-Cre/*Rosa*-tdTomato mice were large (Fig. 1*A*) and

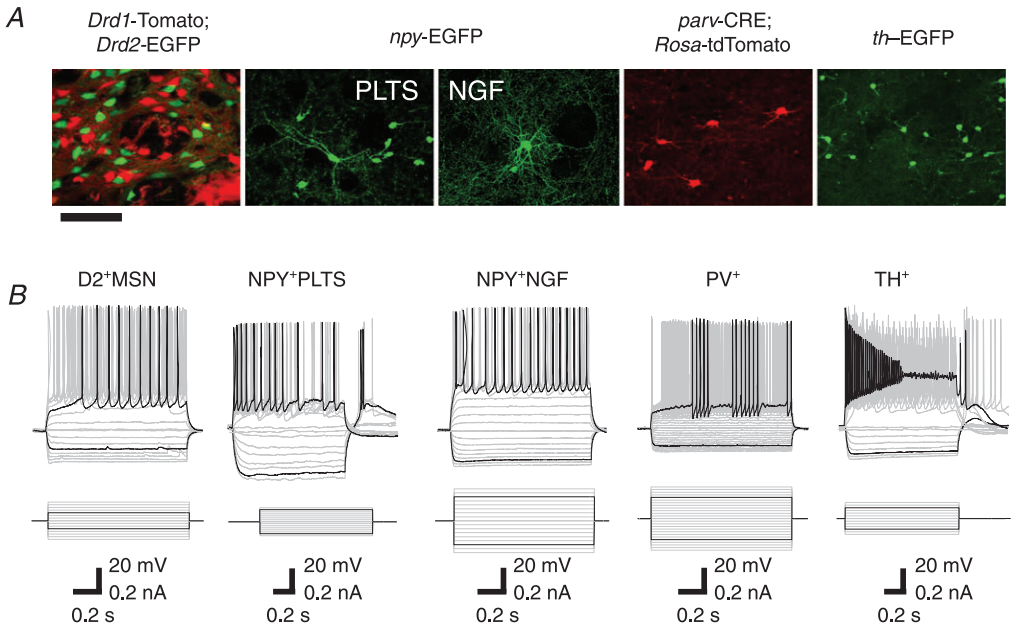

Figure 1. Identification of medium spiny projecting neurones (MSNs) and interneurones
A, fluorescent micrographs identifying populations of MSNs, neuropeptide Y $(NPY)^+$, parvalbumin $(PV)^+$ and tyrosine hydroxylase $(TH)^+$ interneurones in coronal striatal sections of different mice. Scale bar: 100 μm, except for the first panel (70 μm). *B*, electrophysiological characteristics of different striatal neurones during hyperpolarizing and depolarizing current injections. EGFP, enhanced green fluorescent protein; NGF, neurogliaform; PLTS, persistent low-threshold spiking.

fired action potentials at high frequencies with a typical short afterhyperpolarization (Fig. 1*B*; Chang & Kita, 1992; Koós & Tepper, 1999). Interneurones in TH-EGFP mice (Fig. 1*A*) were smaller and had firing patterns (Fig. 1*B*) that often but not always matched that reported by Ibáñez-Sandoval *et al.* (2010). Attempts were not made to subclassify these neurones due to heterogeneity in firing patterns. The majority of NPY^+ PLTS and TH^+ neurones were spontaneously active in cell-attached configuration. Spontaneous firing was never detected in MSNs, NPY^+ NGF or PV^+ interneurones.

Figure 2*A* illustrates the effects of local application of 100 μM CCh + 1 μM Atr (CCh + Atr) on $D2^+$ MSNs in voltage-clamp with high $[Cl^-]_i$ solution, which maximizes detection of GABAergic activity. The cholinergic agonist increased both the holding current as well as the occurrence of sIPSCs in 72 of 94 MSNs (76%), suggesting presynaptic activation of GABAergic neurones via nicotinic ACh receptor (nAChR) leading to increased ambient GABA. CCh + Atr increased sIPSC frequency ($247 \pm 50\%$) and amplitude ($124 \pm 11\%$) in eight $D2^+$ MSNs significantly ($P < 0.05$). Application of 1 μM Atr alone had no effect on the holding current or sIPSCs frequency in all MSNs tested ($n = 24$). As shown in the example of Fig. 2*B*, subsequent application of the $GABA_A$ receptor antagonist BMR (25 μM) blocked the effect of CCh + Atr in 17 MSNs, verifying its GABAergic nature. In four $D2^+$ MSNs, BMR revealed an underlying tonic current, as previously reported (Ade *et al.* 2008). In 4/5 MSNs, TTX (0.5 μM) blocked the effect of CCh + Atr. Figure 2*C* shows a summary plot of CCh + Atr-evoked current comparing $D1^+$, $D2^+$ and unidentified MSNs recorded in mice with fluorescently labelled interneurones. The changes in holding current induced by the cholinergic agonist were not significantly different among these three groups. To test for the presence of endogenous cholinergic tone acting on nicotinic receptors, we locally perfused physostigmine (5 μM) in five $D1^+$ and six $D2^+$ MSNs. The acetylcholinesterase (AChE) inhibitor had no effect on holding current or frequency of sIPSCs. Physostigmine inhibited evoked AMPA-EPSCs in three MSNs, demonstrating its efficacy on cholinergic tone through muscarinic receptors. This effect was completely reversed upon co-application of 1 μM Atr. To further characterize the pharmacology of the nAChR-mediated responses in MSNs, we used the $\alpha4\beta2$-selective antagonist DHβE (10 μM). In 19 unidentified MSNs, the drug had variable effects upon CCh + Atr application, with complete blockade in 14 cells. In the five remaining cells we observed either a partial or no blockade of CCh + Atr-elicited current. Complete blockade of CCh + Atr-evoked currents was seen in 5/5 $D2^+$, but only 5/7 $D1^+$ MSNs. The non-selective nAChR antagonist mecamylamine (60 μM) did not alter holding current, but blocked CCh + Atr-evoked currents in four unidentified MSNs, while the nAChR $\alpha7$ subunit-selective antagonist MLA (50 nM) did not alter holding current or CCh + Atr-evoked currents in five MSNs. To investigate the occurrence of direct cholinergic activation of MSNs, we applied CCh + Atr in the presence of the GABAergic antagonist BMR using potassium gluconate-based internal solution (Fig. 2*D*). From 14 MSNs recorded in this condition, we failed to detect changes in holding current or occurrence of spontaneous synaptic events, demonstrating a lack of nAChR on MSNs. We also investigated if the GABAergic activity seen in MSNs with CCh + Atr could be observed in striatal interneurones. When high $[Cl^-]_i$ solution was used, CCh + Atr increased both the holding current as well as the occurrence of sIPSCs in NPY^+ PLTS and PV^+ interneurones (Fig. 2*E* and *F*), and these responses were significantly reduced by co-application of BMR. This suggests that presynaptic activation of GABAergic interneurones increases inhibition in interneurones similarly to that observed in MSNs.

Application of CCh + Atr to GABAergic interneurones while recording with Kgluc intracellular solution and in the presence of BMR evoked inward currents in most cells tested (Fig. 3*A*). Y-tube drug application to neurones of variable depth in brain slices has limitations that prevented comparison of CCh + Atr response kinetics. However, these responses were always characterized by a remarkable increase in current noise in all responding cells (Fig. 3*A*). The percentage of cells that responded to CCh + Atr in the four groups of interneurones was greater than 60% (53/72 NPY^+ PLTS; 32/33 NPY^+ NGF; 19/26 PV^+; and 60/99 TH^+). Figure 3*B* illustrates the average current recorded in responding cells from the four groups of striatal interneurones. Larger CCh + Atr responses were observed in NPY^+ NGF than in TH^+, NPY^+ PLTS or PV^+ interneurones. As seen in the summary results in Fig. 3*B*, the presence of BMR did not prevent the action of cholinergic drugs in any interneurone group tested. Co-application of CCh + Atr with the voltage-gated Na^+ channel blocker TTX (0.5 μM) produced similar responses in all interneurones (Fig. 3*B*). Similar results were obtained in the presence of the AMPA receptor antagonist NBQX (5 μM, not shown). Our results suggest that subtypes of nAChR are expressed in most striatal GABAergic interneurones. To ascertain for the presence of specific subtypes of nAChRs, we tested the action of nAChR antagonists (Fig. 3*C* and *D*). When CCh + Atr were co-applied with the $\alpha4\beta2$-selective antagonist DHβE (10 μM), current responses were curtailed in all subtypes of interneurones except TH^+. CCh + Atr-evoked currents in eight TH^+ neurones were not affected by the presence of MLA (50 nM). In contrast, when CCh + Atr were co-applied with mecamylamine (60 μM), a use-dependent nAChR blocker, only small currents (<5% control) were observed in all interneurone groups tested.

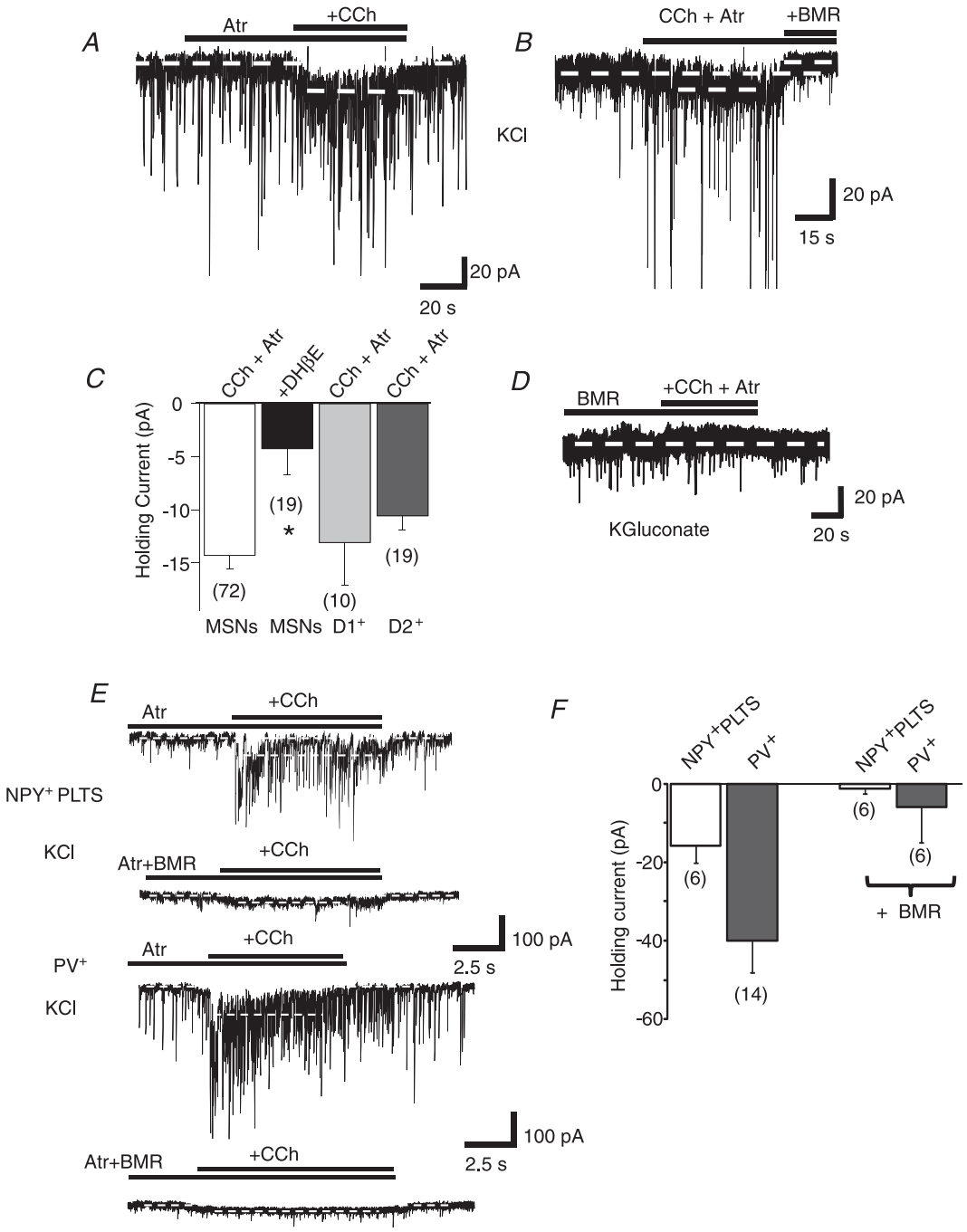

Figure 2. Cholinergic modulation of tonic and phasic GABA current in striatal neurones
Representative traces illustrating the effects of carbachol (CCh; 100 μM) and atropine (Atr; 1 μM) (CCh + Atr, *A* and *B*) on $D2^+$ medium spiny projecting neurones (MSNs) with KCl internal solution. *A*, pre-application of 1 μM Atr failed to alter and did not prevent CCh + Atr-induced changes in the holding current. *B*, application of 25 μM bicuculline methobromide (BMR) unmasked GABAergic tonic current following CCh + Atr-induced changes in the holding current. *C*, bar graph summarizing the changes in holding current induced by CCh + Atr and CCh + Atr + dihydro-β-erythroidine (DHβE) in unidentified MSNs ($^*P < 0.005$). For comparison, changes in holding currents are also shown for $D1^+$ and $D2^+$ MSNs. *D*, changes in GABA-induced holding current were absent when CCh + Atr was applied in BMR with Kgluc internal solution. *E*, representative traces showing the effect of CCh + Atr in the absence and presence of BMR on neuropeptide Y $(NPY)^+$ persistent low-threshold spiking (PLTS) and parvalbumin $(PV)^+$ interneurones while recording with high $[Cl^-]_i$ solution. *F*, bar graph showing the summary of average sustained current in response to CCh + Atr in the presence and absence of BMR in NPY^+ PLTS and PV^+ interneurones.

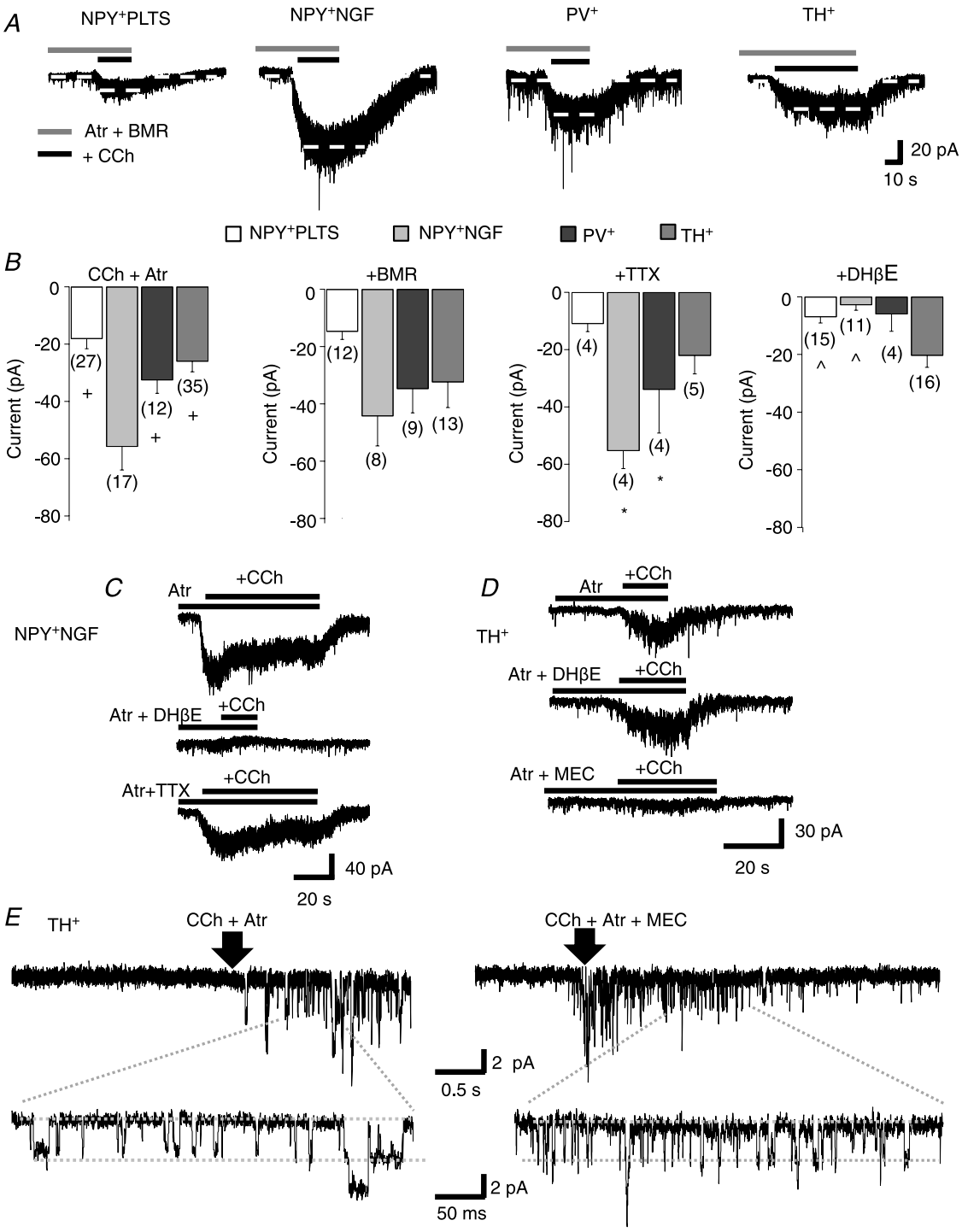

Figure 3. Characteristics of cholinergic response in GABAergic interneurones
A, representative currents elicited by carbachol (CCh) + atropine (Atr) co-applied with bicuculline methobromide (BMR) in neuropeptide Y (NPY)$^+$ persistent low-threshold spiking (PLTS), NPY$^+$ neurogliaform (NGF), parvalbumin (PV)$^+$ and tyrosine hydroxylase (TH)$^+$ interneurones. *B*, summary of current responses recorded in striatal interneurones in the absence and presence of BMR, tetrodotoxin (TTX) or dihydro-β-erythroidine (DHβE) as measured by the lower white dashed line in *A*. *Significance to NPY$^+$ PLTS, +significance to NPY$^+$ NGF, ˆsignificance to TH$^+$. Antagonism of CCh + Atr responses by DHβE compared between an NPY$^+$ NGF (*C*) and a TH$^+$ interneurone (*D*). Note that in (*D*) DHβE failed to block the response in TH$^+$ interneurone that was subsequently blocked by mecamylamine (MEC). *E*, CCh + Atr-elicited channel currents in a patch excised from a TH$^+$ interneurone (left). Co-application with MEC also elicited channel currents (right) in a patch excised from another TH$^+$ interneurone.

To directly demonstrate expression of nAChRs in striatal interneurones, we recorded activation of channel currents upon the application of CCh + Atr to excised outside-out membrane patches. In eight TH^+ neurones we successfully detected channel currents (Fig. 3*E*). Channel current openings were primarily at a main conductance level that averaged 44 ± 1 pS. The mean open time was quite variable between patches (range 2–6 ms) and averaged 3.5 ± 0.7 ms. The open duration decreased significantly when CCh + Atr was co-applied with mecamylamine (Fig. 3*E*, right). Run-down of channel currents in excised patches prevented proper pharmacological analysis. These results are comparable to previous reports characterizing functional properties of neuronal nAChR channels in interneurones and transfected cells (Ragozzino *et al*. 1997; Shao & Yakel, 2000), and suggest that both $\beta 2$ and $\beta 4$ subunit-containing nAChRs can be found in striatal TH^+ interneurones. To further investigate this possibility, we studied the action of cytisine, a partial agonist of $\beta 2$ and full agonist of $\beta 4$ subunit-containing nAChRs (Zoli *et al.* 1998). Using 10 μM cytisine, we detected responses in 3/5 NPY^+ PLTS cells (3.3 ± 0.9 pA) and in 2/4 PV^+ cells (13.2 ± 8.4 pA). Cytisine-evoked current was significantly larger in 7/7 TH^+ cells (19.4 ± 6.9 pA) than in other interneurones. We also studied 10 μM cytosine-induced currents in four $D2^+$ MSNs. Cytisine increased sIPSC frequency ($216 \pm 38\%$) and amplitude ($129 \pm 4\%$), and induced a sustained current of 11.0 ± 1.4 pA. Taken together our results strongly suggest the presence of nAChR in striatal interneurones, but not MSNs.

To examine cholinergic control of striatal interneurones, we studied the effects of CCh + Atr using cell-attached recordings. We studied TH^+ and NPY^+ PLTS as they are often spontaneously active and therefore likely to be involved in generating ambient GABA. In 5/6 TH^+ neurones and in 4/9 NPY^+ PLTS, CCh + Atr increased action potential firing. Interestingly, CCh + Atr application decreased firing in three NPY^+ PLTS, and failed to have an effect on one TH^+ and one NPY^+ PLTS. These variable results were likely due to the fact that some interneurones do not respond to CCh + Atr. In these non-responding neurones, spontaneous firing is likely suppressed via GABAergic activation by CCh + Atr. This suggests that cholinergic activation of GABAergic interneurones will depend on a balance between the presence of nAChR and the extent and strength of GABAergic innervations from other interneurones. To better control these variables, we used current-clamp recordings with Kgluc-based intracellular solution. These experiments were performed in interneurones at their resting membrane potential (RMP). As shown in the examples in Fig. 4*A*, NPY^+ PLTS and TH^+ were often spontaneously active at RMP. However, NPY^+ NGF and PV^+ cells that had more negative RMPs were not. Examples in Fig. 4*A* and the summary results in Fig. 4*B* illustrate that CCh + Atr promoted action potential firing in most interneurones, although the extent of depolarization varied (Fig. 4*C*). In PV^+ interneurones, however, CCh + Atr depolarization induced firing only when intracellular KCl was used (Fig. 4*A*, bottom right). CCh + Atr-induced firing in PV^+ interneurones was blocked by BMR (Fig. 4*A*, bottom right and *B*). This suggests that when Kgluc solution is used, the strong inhibitory input onto PV^+ interneurones elicited by CCh + Atr (Fig. 1*E*) counterbalances the direct depolarization via nAChR preventing action potential firing.

To further investigate the role of distinct GABAergic interneurones in generating persistent GABAergic conductance in MSNs, we performed dual recordings (Fig. 5) from unidentified MSNs, and 44 TH^+, nine PV^+, 50 NPY^+ NGF and 15 NPY^+ PLTS interneurones. Figure 5*A* shows representative traces from dual voltage-clamp recordings between synaptically connected interneurone–MSN pairs. From a holding potential of −70 mV, presynaptic GABAergic interneurones were briefly depolarized to 0 mV to evoke neurotransmitter release. Simultaneously, MSNs were voltage-clamped at −70 mV while using high $[Cl^-]_i$ solution that allowed reliable detection of inhibitory synaptic connectivity. Connectivity was observed in all interneurone groups tested (Fig. 5*B*), except for NPY^+ PLTS cells that have been reported to have low connectivity with MSNs, as reported previously (Gittis *et al*. 2010). The use of internal Kgluc solution in interneurones prevented detection of reciprocal GABAergic synapses with MSNs. Figure 5*C* summarizes the average peak IPSC amplitude measured in interneurone–MSN pairs. Large variability of IPSC size was seen between pairs, and the average values were not significantly different between interneurone groups. As recently reported, presynaptic NPY^+ NGF interneurones produced longer lasting IPSCs in MSNs (Fig. 5*A* top; English *et al.* 2011; Ibáñez-Sandoval *et al.* 2011). We also studied synaptic connectivity upon higher frequency stimulation of the presynaptic interneurones by eliciting 10 depolarizing steps to 0 mV at 20 Hz (Fig. 5*A*, bottom). We observed robust synaptic activity shown as summating IPSCs and increased baseline holding current. Figure 5*D* summarizes the size of the baseline current elicited by stimulation at 20 Hz. The baseline current shift was significantly larger for NPY^+ NGF neurones, consistent with the slow kinetics of IPSCs produced in MSNs.

We then extended the use of dual recordings to measure the sustained activation of GABAergic current in MSNs while recording from presynaptic interneurones in current-clamp in a more physiological condition. As shown in the examples in Fig. 6*A*, presynaptic interneurone activation generated summating IPSCs and increased baseline holding current in connected MSNs. When presynaptic firing rates were less than 5 Hz, the MSN baseline current shift was evident for synaptically

connected NPY$^+$ NGF interneurones (21.6 ± 4.5 pA, $n = 5$). When TH$^+$ interneurones were synaptically connected to MSNs, the baseline current shift induced by low-frequency firing was occasionally seen, but it depended strongly on the strength of connectivity. Using the same recording configuration, we applied CCh + Atr and compared the currents induced in MSNs. MSNs synaptically coupled to NPY$^+$ NGF or TH$^+$ interneurones (Fig. 6*B*, top) displayed increased sIPSC frequency and holding current upon CCh + Atr application. However, these changes in conductance always occurred before action potential firing in the presynaptic interneurone in all pairs tested, regardless of synaptic connectivity, suggesting contributions from other presynaptic interneurones. This is supported by the action of CCh + Atr shown in the recording in Fig. 6*B*, bottom, from a

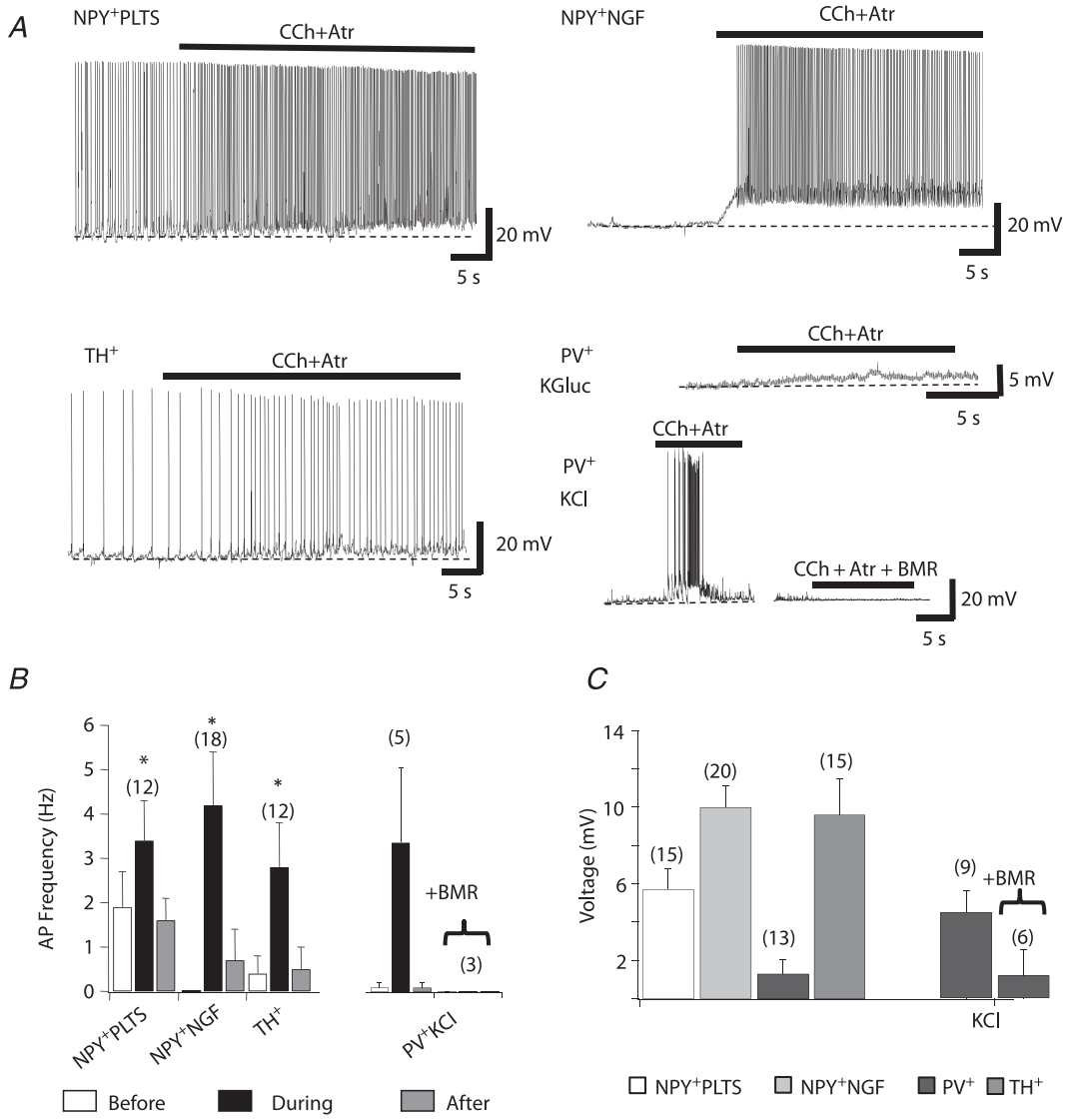

Figure 4. Cholinergic agonists elicit action potentials (APs) in striatal interneurones
A, representative traces showing effects of carbachol (CCh) + atropine (Atr) on firing activity of neuropeptide Y (NPY)$^+$ persistent low-threshold spiking (PLTS), NPY$^+$ neurogliaform (NGF), parvalbumin (PV)$^+$ and tyrosine hydroxylase (TH)$^+$ interneurones with Kgluc internal solution. Cells were recorded at RMP. CCh + Atr produced a small depolarization in a PV$^+$ interneurone with Kgluc internal solution. In contrast with KCl internal solution, an initially quiescent PV$^+$ interneurone responded with a burst of APs that was blocked by bicuculline methobromide (BMR). *B*, bar graph summarizing AP frequency in striatal interneurones before, during and after application of CCh + Atr (left). Bar graph summarizing AP frequency in PV$^+$ interneurones measured using high $[Cl^-]_i$ solution before, during and after application of CCh + Atr in the presence and absence of BMR (right). *C*, bar graph summarizing membrane depolarization in striatal interneurones upon application of CCh + Atr. Data from PV$^+$ interneurones recorded in Kgluc (left) are compared with high $[Cl^-]_i$ solution recordings (right) in the presence and absence of BMR.

non-connected NPY$^+$ PLTS and MSN pair. When the cells were synaptically connected there was a considerable increase in holding current in the MSN that correlated to presynaptic action potential firing in the interneurone (Fig. 7*A*). This is highlighted by the reduction in holding current in MSNs when presynaptic interneurones (NPY$^+$ NGF, Fig. 7*A*; and TH$^+$, Fig. 7*B*) were hyperpolarized during the application of CCh + Atr. Taken together, these results show that cholinergic activation of GABAergic interneurones generates a cloud of GABA that evokes sustained current and regulates the excitability of MSNs. However, synaptically connected interneurones can take advantage of this mechanism and directly influence the firing pattern of connected MSNs.

Discussion

Our study demonstrates that nicotinic receptor agonists directly excite striatal GABAergic interneurones through feedforward activation of TH$^+$ and NPY$^+$ NGF interneurones. When nicotinic agonists were applied in whole-cell voltage-clamp, MSNs responded with a shift in holding current accompanied by increased amplitude and frequency of sIPSCs. This response was suppressed by both BMR and TTX, indicating it was GABA- and action potential-mediated. Nicotinic receptor stimulation has been reported to elicit TTX-insensitive GABAergic synaptic currents in rat MSNs (Liu *et al*. 2007). We do not know the reason for the discrepancy other than the difference in species. Our findings that MSNs do not respond directly to nicotinic agonists preclude contribution from MSN collaterals and identify GABAergic interneurones as their primary source of GABA during nicotinic activation. Indeed, all four major classes of striatal GABAergic interneurones are activated directly by nicotinic agonists. However, the degree and consistency of activation is most prominent in the NGF subtype of NPY$^+$ interneurones. This finding

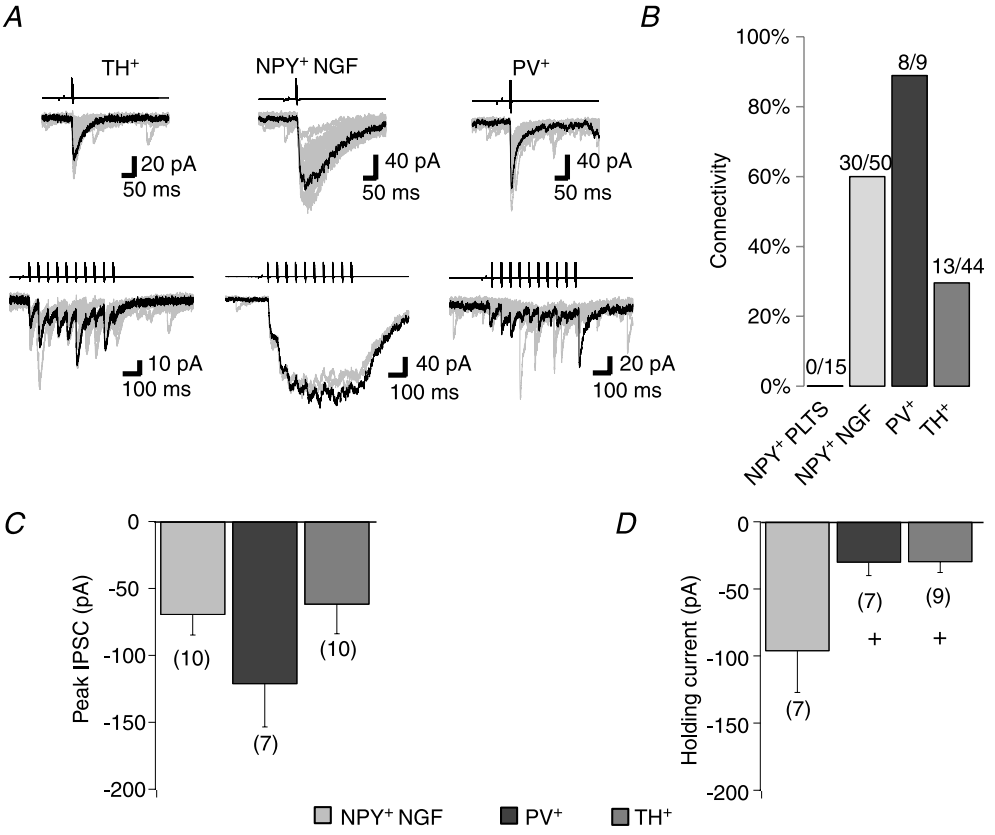

Figure 5. Characterization of GABA current in synaptically connected pairs of interneurones and MSNs
A (top), representative traces from synaptically connected pairs of a presynaptic tyrosine hydroxylase (TH)$^+$, neuropeptide Y (NPY)$^+$ neurogliaform (NGF) or parvalbumin (PV)$^+$ interneurone and a postsynaptic MSN. A depolarization step to +40 mV (4 ms in duration) in either a TH$^+$ or a PV$^+$ interneurone induced a typical rapidly decaying IPSC in the MSNs, but in a NPY$^+$ NGF interneurone, it induced an IPSC with slow rise and decay kinetics (bottom). When the same presynaptic interneurones were given a train of 10 depolarizations (4 ms to +40 mV) at 20 Hz, the MSN innervated by an NPY$^+$ NGF interneurone responded with a steady change in current. *B*, bar graph summarizing the percentage synaptic connectivity of attempted dual recordings between presynaptic interneurones and postsynaptic MSNs. The peak response from single IPSCs (*C*) and baseline current changes (*D*) are summarized. PLTS, persistent low-threshold spiking.

correlates well with a recent report by English *et al.* (2011) that implicates NPY$^+$ NGF interneurones as key mediators of striatal cholinergic responses. In addition, our data show that in the acute slice preparation, all interneurone classes tested here have nAChR and, except NPY$^+$ PLTS, make detectable synaptic connections with MSNs. Therefore, interneurones contribute to the pharmacologically induced nicotinic response in MSNs, albeit with distinct roles. Functional nAChRs have also been reported on interneurones in the rat hippocampus (Jones & Yakel, 1997), demonstrating that they are a common feature of a large group of these cell types (Lee *et al.* 2010). Previous studies have shown a dual cholinergic control of PV$^+$ interneurones in the neostriatum (Koós & Tepper, 2002). However, our results and those of English *et al.* (2011) suggest that although PV$^+$ interneurones express nAChRs they cannot be easily activated by cholinergic agonists.

Pharmacological investigation of currents induced by CCh in the presence of Atr in distinct stratial neurones strongly suggested the involvement of different receptor subtypes. For instance, sensitivity of currents to DHβE in NPY$^+$ and PV$^+$ interneurones implicates the expression of $\alpha4\beta2$ nAChRs, the predominant subtype in the CNS. In contrast, currents in TH$^+$ interneurones were largely insensitive to DHβE and MLA, although blocked by mecamylamine. This suggests a possible role of the $\alpha3\beta4$ receptor in these neurons, as supported by the sensitivity to cytisine, a preferred agonist at these receptors (Zoli *et al.* 1998). Importantly when evaluating the action of nAChR antagonists on cholinergic-induced GABA responses in MSNs, we

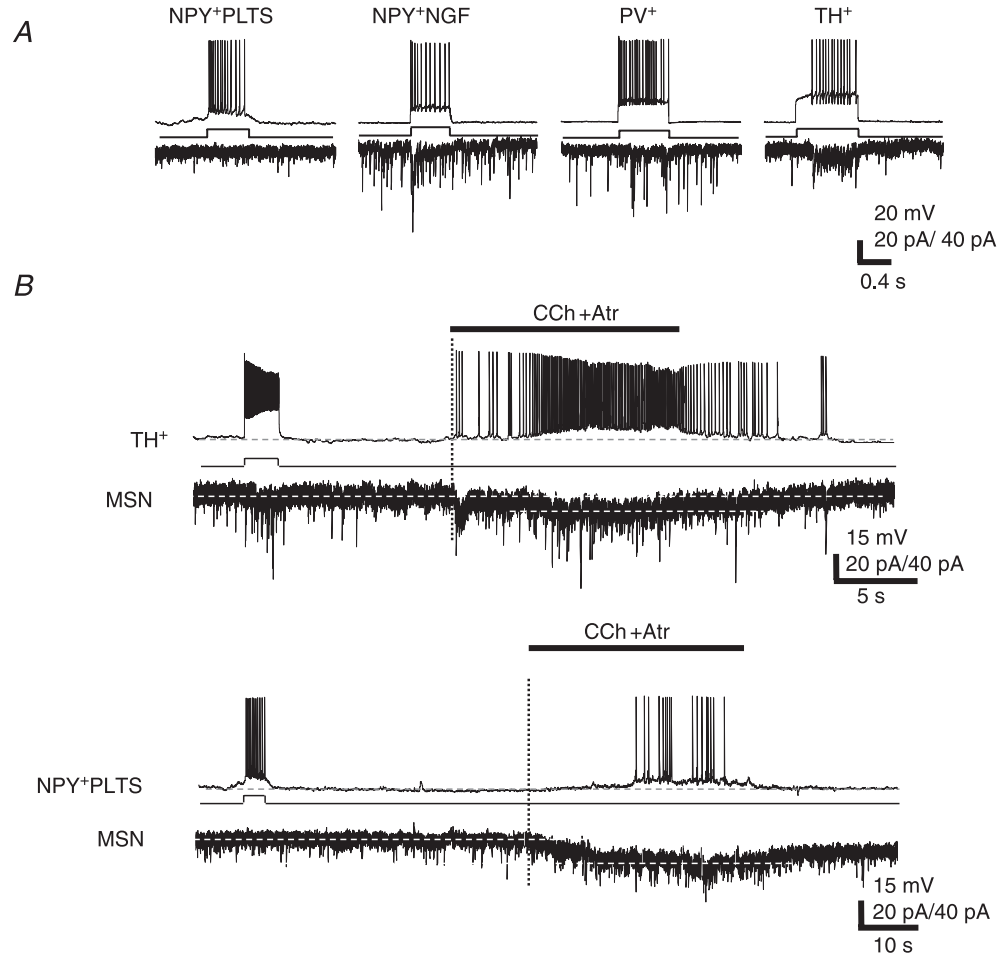

Figure 6. Representative traces of paired recordings between medium spiny projecting neurones (MSNs) and distinct interneurones
A, presynaptic interneurone action potentials in response to depolarizing current injections elicited GABAergic currents only in synaptically coupled postsynaptic MSNs. Action potential frequency was <5 Hz in all examples. *B*, a comparison of GABAergic currents following presynaptic current injections with perfusion of carbachol (CCh) + atropine (Atr) in a tyrosine hydroxylase (TH)$^+$/MSN (top) and a neuropeptide Y (NPY)$^+$ persistent low threshold spiking (PLTS)/MSN pair (bottom). Note the NPY$^+$ PLTS/MSN pair was not synaptically coupled, while the TH$^+$/MSN pair was. CCh + Atr elicited currents in postsynaptic MSNs in both situations occurred before presynaptic action potential firing.

observed considerable heterogeneity. This suggests that MSNs receive GABAergic innervation from different interneurone populations, which may be competing to mediate nicotinic regulation of MSN output. Further experiments are needed to address receptor subtype using more specific pharmacological tools (when available) and transgenic mice with deletions of specific subunits. Our results do, however, begin to delineate the complexity in striatal interneurone regulation in which a mosaic of receptor subtypes is expressed to modulate intrinsic striatal network.

Previous studies reported the existence of a tonic GABA current in MSNs in acute striatal slices (Ade *et al*. 2008; Santhakumar *et al*. 2010; Janssen *et al*. 2011). As this current was blocked or significantly decreased by TTX, tonic current is likely generated by spontaneously firing GABAergic interneurones. In our study we investigated the relationship between GABAergic tonic current and the sustained GABAergic current induced by cholinergic activation of the striatal network via nAChR. Perfusion with an AChE inhibitor and a non-specific blocker of nAChR both failed to alter tonic current. Therefore, endogenous nicotinic cholinergic activity is not robust in our slices. In addition, our results show that the interneurone subtypes most sensitive to nAChR agonists do not display spontaneous firing. Lastly, CCh + Atr-induced current did not differ between $D1^+$ and $D2^+$ MSNs. Thus, the tonic and the cholinergic agonist-induced GABA currents have different origins. In addition, tonic current must derive from striatal interneurones that exhibit spontaneous activity including subtypes of the TH^+ and the NPY^+ PLTS neurones, but are not necessarily involved in cholinergic regulation of striatal output. One should consider, however, our findings that nAChRs powerfully

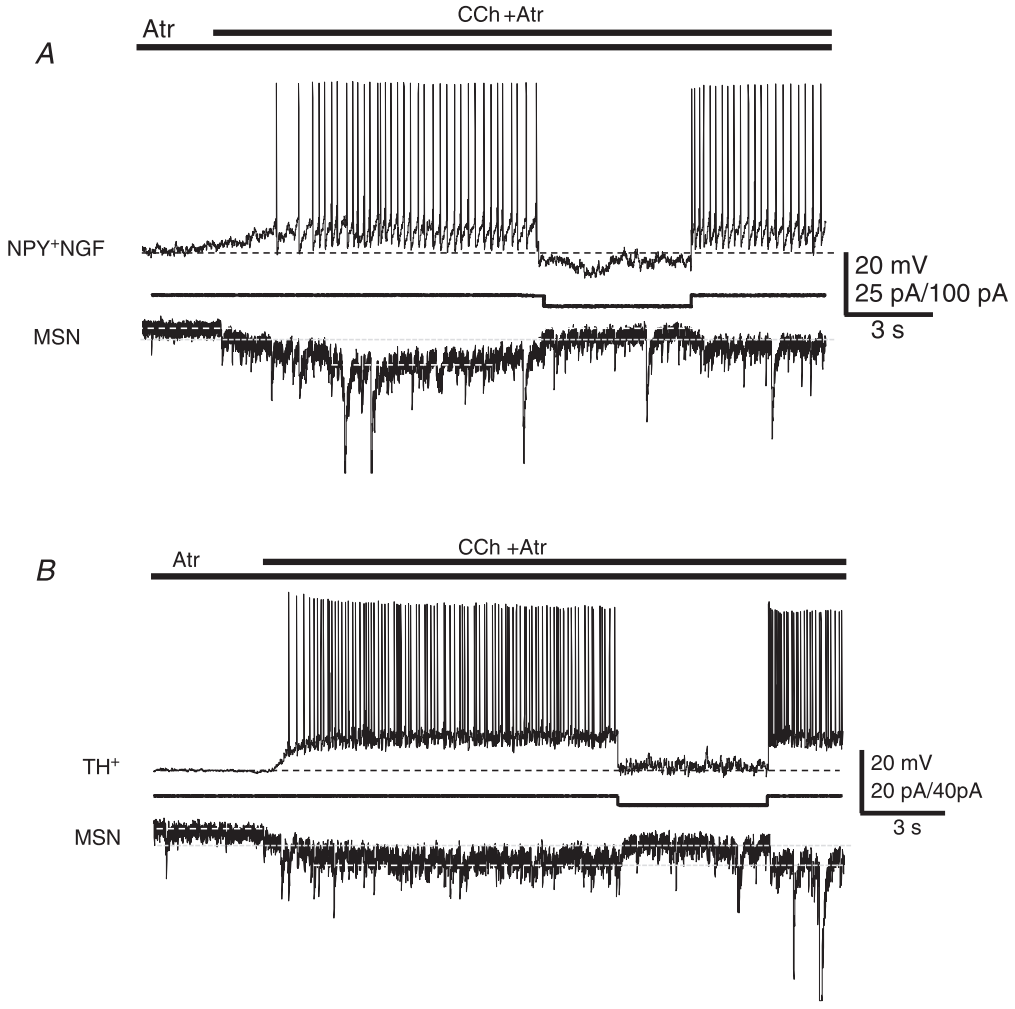

Figure 7. Action potential firing in presynaptic interneurones contributes to sustained GABA current in medium spiny projecting neurones (MSNs)
Presynaptic hyperpolarization cessation of carbachol (CCh) + atropine (Atr)-induced action potential firing decreased postsynaptic response in both a neuropeptide Y $(NPY)^+$ neurogliaform (NGF)/MSN (*A*) and a tyrosine hydroxylase $(TH)^+$/MSN pair (*B*).

regulate interneurone firing rates to produce additional GABAergic conductance, which may fulfill diverse roles in striatal control of movements.

Recordings from connected neurones also confirmed the observation in English *et al.* (2011) that NPY^+ NGF interneurones form synapses with and generate IPSCs in MSNs with slow rise and decay kinetics. The slow IPSCs facilitate summation to generate a persistent GABA conductance in MSNs when action potential firing in presynaptic NPY^+ NGF interneurones is sustained at low frequencies (<5 Hz). Similarly, subtypes of TH^+ but not NPY^+ PLTS interneurones can also produce sustained GABAergic conductance in MSNs. This is in contrast to PV^+ interneurones that will require higher presynaptic firing rate.

$D2^+$ MSNs have larger tonic current due to their greater sensitivity to GABA (Ade *et al.* 2008). In the present study we observed that GABAergic response to nicotinic activation of presynaptic GABAergic interneurones is similar between $D1^+$ and $D2^+$ MSNs. This suggests the possibility of a preferential targeting of striatopallidal and striatonigral MSNs by specific interneurones (Gittis *et al.* 2010).

Optogenetic control of cholinergic interneurones *in vivo* and *in vitro* has demonstrated the regulation of MSN firing via GABAergic mechanisms (Witten *et al.* 2010; English *et al.* 2011). Our results extend the evidence of nAChR in additional subtypes of striatal interneurones. Thus, nicotinic activation of these interneurones generates GABAergic tonic and phasic conductances in MSNs that regulate striatal output. Additional optogenetic studies also show that synchronous cholinergic neurone activation can directly gate the release of dopamine via nAChR on dopaminergic terminals (Cachope *et al.* 2012; Threlfell *et al.* 2012). The theory of ACh dopamine imbalance is widely regarded as a fundamental cause in various basal ganglia disorders (Surmeier & Graybiel, 2012). Dehorter *et al.* (2009) showed that chronic dopamine depletion induced increased occurrence of large-amplitude IPSC bursts in MSNs. The Dehorter *et al.* study suggests that striatal interneurones other than PV^+ mediated this effect. It will be important to establish the changes that occur in cholinergic regulation of striatal function with dopamine depletion in animal models of basal ganglia disorders.

References

Ade KK, Janssen MJ, Ortinski PI & Vicini S (2008). Differential tonic GABA conductances in striatal medium spiny neurons. *J Neurosci* **28**, 1185–1197.

Azdad K, Chàvez M, Don Bischop P, Wetzelaer P, Marescau B, De Deyn PP, Gall D & Schiffmann SN (2009). Homeostatic plasticity of striatal neurons intrinsic excitability following dopamine depletion. *PLoS One* **4**, e6908.

Beatty J, Sullivan M, Morikawa H & Wilson CJ (2012). Complex autonomous firing patterns of striatal low-threshold spike interneurons. *J Neurophysiol* **108**, 771–781.

Bennett BD & Wilson CJ (1999). Spontaneous activity of neostriatal cholinergic interneurons in vitro. *J Neurosci* **19**, 5586–5596.

Bonsi P, Cuomo D, Martella G, Madeo G, Schirinzi T, Puglisi F, Ponterio G & Pisani A (2011). Centrality of striatal cholinergic transmission in basal ganglia function. *Front Neuroanat* **5**, 6.

Burkhardt JM, Jin X & Costa RM (2009). Dissociable effects of dopamine on neuronal firing rate and synchrony in the dorsal striatum. *Front Integr Neurosci* **3**, 1–12.

Cachope R, Mateo Y, Mathur BN, Irving J, Wang HL, Morales M, Lovinger DM & Cheer JF (2012). Selective activation of cholinergic interneurons enhances accumbal phasic dopamine release: setting the tone for reward processing. *Cell Rep* **2**, 33–41.

Calabresi P, Centonze D, Gubellini P, Pisani A & Bernardi G (2000). Acetylcholine-mediated modulation of striatal function. *Trends Neurosci* **23**, 120–126.

Chang HT & Kita H (1992). Interneurons in the rat striatum: relationships between parvalbumin neurons and cholinergic neurons. *Brain Res* **574**, 307–311.

de Rover M, Lodder JC, Kits KS, Schoffelmeer ANM & Brussaard AB (2002). Cholinergic modulation of nucleus accumbens medium spiny neurons. *Eur J Neurosci* **16**, 2279–2290.

Dehorter N, Guigoni C, Lopez C, Hirsch J, Eusebio A, Ben-Ari Y & Hammond C (2009). Dopamine-deprived striatal GABAergic interneurons burst and generate repetitive gigantic IPSCs in medium spiny neurons. *J Neurosci* **29**, 7776–7787.

Drenan RM, Grady SR, Steele AD, McKinney S, Patzlaff NE, McIntosh JM, Marks MJ, Miwa JM & Lester H (2010). Cholinergic modulation of locomotion and striatal dopamine release is mediated by alpha6alpha4* nicotinic acetylcholine receptors. *J Neurosci* **30**, 9877–9889.

English DF, Ibáñez-Sandoval O, Stark E, Tecuapetla F, Buzsáki G, Deisseroth K, Tepper JM & Koós T (2011). GABAergic circuits mediate the reinforcement-related signals of striatal cholinergic interneurons. *Nat Neurosci* **15**, 123–130.

Fino E, Glowinski J & Venance L (2007). Effects of acute dopamine depletion on the electrophysiological properties of striatal neurons. *Neurosci Res* **58**, 305–316.

Forcelli PA, Janssen MJ, Vicini S & Gale K (2012). Neonatal exposure to antiepileptic drugs disrupts striatal synaptic development. *Ann Neurol* **72**, 363–372.

Gerfen CR, Engber TM, Mahan LC, Susel Z, Chase TN, Monsma FJ Jr & Sibley DR (1990). D1 and D2 dopamine receptor-regulated gene expression of striatonigral and striatopallidal neurons. *Science* **250**, 1429–1432.

Gittis AH, Nelson AB, Thwin MT, Palop JJ & Kreitzer AC (2010). Distinct roles of GABAergic interneurons in the regulation of striatal output pathways. *J Neurosci* **30**, 2223–2234.

Gong S, Zheng C, Doughty ML, Losos K, Didkovsky N, Schambra UB, Nowak NJ, Joyner A, Leblanc G, Hatten ME & Heintz N (2003). A gene expression atlas of the central nervous system based on bacterial artificial chromosomes. *Nature* **425**, 917–925.

Graybiel AM, Aosaki T, Flaherty AW & Kimura M (1994). The basal ganglia and adaptive motor control. *Science* **265**, 1826–1831.

Hevers W & Luddens H (2002). Pharmacological heterogeneity of gamma-aminobutyric acid receptors during development suggests distinct classes of rat cerebellar granule cells in situ. *Neuropharmacology* **42**, 34–47.

Ibáñez-Sandoval O, Tecuapetla F, Unal B, Shah F, Koós T & Tepper JM (2010). Electrophysiological and morphological characteristics and synaptic connectivity of tyrosine hydroxylase-expressing neurons in adult mouse striatum. *J Neurosci* **30**, 6999–7016.

Ibáñez-Sandoval O, Tecuapetla F, Unal B, Shah F, Koós T & Tepper JM (2011). A novel functionally distinct subtype of striatal neuropeptide Y interneuron. *J Neurosci* **31**, 16757–16769.

Jáidar O, Carrillo-Reid L, Hernández A, Drucker-Colín R, Bargas J & Hernández-Cruz A (2010). Dynamics of the Parkinsonian striatal microcircuit: entrainment into a dominant network state. *J Neurosci* **30**, 11326–11336.

Janssen MJ, Ade KK, Fu Z & Vicini S (2009). Dopamine modulation of GABA tonic conductance in striatal output neurons. *J Neurosci* **29**, 5116–5126.

Janssen MJ, Yasuda RP & Vicini S (2011). $GABA_{(A)}$ receptor $\beta 3$ subunit expression regulates tonic current in developing striatopallidal medium spiny neurons. *Front Cell Neurosci* **5**, 15.

Jones S & Yakel JL (1997). Functional nicotinic ACh receptors on interneurons in the rat hippocampus. *J Physiol* **504**, 603–610.

Kawaguchi Y (1993). Physiological, morphological, and histochemical characterization of three classes of interneurons in rat neostriatum. *J Neurosci* **13**, 4908–4923.

Koós T & Tepper JM (1999). Inhibitory control of neostriatal projection neurons by GABAergic interneurons. *Nat Neurosci* **2**, 467–472.

Koós T & Tepper JM (2002). Dual cholinergic control of fast-spiking interneurons in the neostriatum. *J Neurosci* **22**, 529–535.

Kreitzer AC (2009). Physiology and pharmacology of striatal neurons. *Annu Rev Neurosci* **32**, 127–147.

Lee S, Hjerling-Leffler J, Zagha E, Fishell G & Rudy B (2010). The largest group of superficial neocortical GABAergic interneurons expresses ionotropic serotonin receptors. *J Neurosci* **30**, 16796–16808.

Liu Z, Otsu Y, Vasuta C, Nawa H & Murphy TH (2007). Miniature synaptic transmission mediated by nicotinic stimulation of immature striatal action-potential-independent GABAergic tone. *J Neurophysiol* **98**, 581–593.

Madisen L, Zwingman TA, Sunkin SM, Oh SW, Zariwala HA, Gu H, Ng LL, Palmiter RD, Hawrylycz MJ, Jones AR, Lein ES & Zeng H (2010). A robust and high-throughput Cre reporting and characterization system for the whole mouse brain. *Nat Neurosci* **13**, 133–140.

Murase K, Ryu PD & Randic M (1989). Excitatory and inhibitory amino acids and peptide-induced responses in acutely isolated rat spinal dorsal horn neurons. *Neurosci Lett* **103**, 56–63.

Murray AJ, Sauer JF, Riedel G, McClure C, Ansel L, Cheyne L, Bartos M, Wisden W & Wulff P (2011). Parvalbumin-positive CA1 interneurons are required for spatial working but not for reference memory. *Nat Neurosci* **14**, 297–279.

Ortinski PI, Lu C, Takagaki K, Fu Z & Vicini S (2004). Expression of distinct alpha subunits of GABAA receptor regulates inhibitory synaptic strength. *J Neurophysiol* **92**, 1718–1727.

Partridge JG, Janssen MJ, Chou DYT, Abe K, Zukowska Z & Vicini S (2009). Excitatory and inhibitory synapses in neuropeptide Y-expressing striatal interneurons. *J Neurophysiol* **102**, 3038–3045.

Pisani A, Bernardi G, Ding J & Surmeier DJ (2007). Re-emergence of striatal cholinergic interneurons in movement disorders. *Trends Neurosci* **30**, 545–553.

Ragozzino D, Fucile S, Giovannelli A, Grassi F, Mileo AM, Ballivet M, Alemà S & Eusebi F (1997). Functional properties of neuronal nicotinic acetylcholine receptor channels expressed in transfected human cells. *Eur J Neurosci* **9**, 480–488.

Santhakumar V, Jones RT & Mody I (2010). Developmental regulation and neuroprotective effects of striatal tonic $GABA_A$ currents. *Neuroscience* **167**, 644–655.

Shao Z & Yakel JL (2000). Single channel properties of neuronal nicotinic ACh receptors in stratum radiatum interneurons of rat hippocampal slices. *J Physiol* **527**, 507–513.

Shuen JA, Chen M, Gloss B & Calakos N (2008). Drd1a-tdTomato BAC transgenic mice for simultaneous visualization of medium spiny neurons in the direct and indirect pathways of the basal ganglia. *J Neurosci* **28**, 2681–2685.

Sullivan M, Chen H & Morikawa H (2008). Recurrent inhibitory network among striatal cholinergic interneurons. *J Neurosci* **28**, 8682–8690.

Surmeier DJ & Graybiel AM (2012). A feud that wasn't: acetylcholine evokes dopamine release in the striatum. *Neuron* **75**, 1–3.

Threlfell S, Lalic T, Platt NJ, Jennings KA, Deisseroth K & Cragg SJ (2012). Striatal dopamine release is triggered by synchronized activity in cholinergic interneurons. *Neuron* **75**, 58–64.

Wilson CJ, Chang HT & Kitai ST (1990). Firing patterns and synaptic potentials of identified giant aspiny interneurons in the rat neostriatum. *J Neurosci* **10**, 508–519.

Witten IB, Lin S-C, Brodsky M, Prakash R, Diester I, Anikeeva P, Gradinaru V, Ramakrishnan C & Deisseroth K (2010). Cholinergic interneurons control local circuit activity and cocaine conditioning. *Science* **330**, 1677–1681.

Zhou FM, Wilson CJ & Dani J (2002). Cholinergic interneuron characteristics and nicotinic properties in the striatum. *J Neurobiol* **53**, 590–605.

Zoli M, Léna C, Picciotto MR & Changeux JP (1998). Identification of four classes of brain nicotinic receptors using beta2 mutant mice. *J Neurosci* **18**, 4461–4472.

Author contributions

R.L., M.J.J., J.G.P. and S.V. contributed to the conception and design of the study, performed the experiments, analysed data, prepared figures, drafted the manuscript, edited and revised the manuscript. All authors approved the final version of the manuscript.

Acknowledgements

We thank Dr David Lovinger from the National Institute on Alcohol Abuse and Alcoholism for providing the BAC-*drd2*-EGFP mice; Dr Nicole Calakos from Duke University for providing the BAC-*drd1a*-tdTomato mice; and Dr David Sulzer from Columbia University and Dr Kathy Maguire-Zeiss from Georgetown University for providing *th*-EGFP mice. This study was supported by: NIH grant MH64797.

Translational perspective

ACh and GABA are critically important to the striatum, and to the functions of the basal ganglia in health and disease. Our finding of specific and distinct nicotinic cholinergic regulation of striatal interneurone subtypes offers a new window on a key mechanism of striatal processing and novel therapeutic opportunities.